SEMARAK ILMU PUBLISHING

Journal of Advanced Research in Fluid Mechanics and Thermal Sciences

Journal homepage:
https://semarakilmu.com.my/journals/index.php/fluid_mechanics_thermal_sciences/index
ISSN: 2289-7879

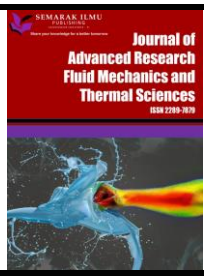

Implementation of Interleaved Converter for Fast Charging Stations

Arigela Satya Veerendra[1,*], Kambampati Lakshmi[2], Chavali Punya Sekhar[3], Sivayazi Kappagantula[4], Kumaran Kadirgama[5,6,7], Norazlianie Sazali[7,8]

[1] Department of Electrical and Electronics Engineering, Manipal Institute of Technology, Manipal Academy of Higher Education, Manipal, 576104, India
[2] Department of Electrical and Electronics Engineering, Aditya College of Engineering and Technology, Surampalem, India
[3] Department of Electrical and Electronics Engineering, Acharya Nagarjuna University, Guntur, India
[4] Department of Mechatronics, Manipal Institute of Technology, Manipal Academy of Higher Education, Manipal, 576104, India
[5] Faculty of Mechanical and Automotive Engineering Technology, Universiti Malaysia Pahang, 26600 Pekan, Malaysia
[6] College of Engineering, Almaaqal University, Basra, 61003, Iraq
[7] Centre of Excellence for Advanced Research in Fluid Flow (CARIFF), Universiti Malaysia Pahang Al-Sultan Abdullah, Lebuhraya Tun Razak, Gambang, Kuantan, Pahang, Malaysia
[8] Faculty of Manufacturing and Mechatronic Engineering Technology, University Malaysia Pahang, 26600 Pekan, Pahang, Malaysia

ARTICLE INFO

Article history:
Received 12 July 2024
Received in revised form 24 October 2024
Accepted 5 November 2024
Available online 20 November 2024

Keywords:
Charging infrastructure; interleaved boost converter; battery; electric vehicle; smart grid

ABSTRACT

The major goals of this effort are to create an electric vehicle charging station microgrid that combines the utility grid, a solar PV plant, and a bioenergy system as its primary energy sources. Here, the solar system is designed for 15kW, and the energy system is designed for 5kW. To improve the efficiency and maximize the performance of the distributed energy system, a DC-DC converter-based perturb and observe MPPT technique is implemented. The proposed arrangement makes it possible to build a microgrid that is effective, affordable, and distinctively local. The utilization range of electric vehicles is increasing rapidly and still in some areas it is limited due to more charging times. This can be improved by providing fast charging conditions that enable charging a vehicle in less time. To maintain these fast-charging conditions, an efficient, compact-sized DC-DC converter with high power output is required. This paper introduces an interleaved DC-DC power converter to meet the above requirements. The proposed interleaved multi-phase converter, which is part of fast charging stations, can charge the electric vehicle in less than 3 hours. To achieve high power density, ripple reduction on the output current and to improve the efficiency of the converter a space vector modulation technique is applied. The operation of an interleaved converter is analysed theoretically. Simulation analysis of the proposed interleaved power converter shows the good behaviour of the converter and charging conditions of various electric vehicle systems.

* *Corresponding author.*
E-mail address: veerendra.babu@manipal.edu

https://doi.org/10.37934/arfmts.124.1.128143

1. Introduction

Over the past ten years, there has been an increase in the use of fossil fuels and pollution issues in automobiles. Automobile manufacturers presented electric vehicles as a solution to these issues. Both in the transient and peak stages, batteries have to provide power but, the cost and weight of batteries become a severe problem for batteries. Supercapacitors and fuel cells have been employed to address battery-related issues [1]. In order to address the issue of battery-operated EVs' inadequate storage, hybrid and plug-in electric vehicles have been introduced [2]. Revolutionizing mobility through electric vehicles (EVs) necessitates a robust charging infrastructure. In India, the EV charging infrastructure is rapidly expanding, with a focus on charging specifications, standards, regulations, and government initiatives [3].

The suggested single-stage converter covered in the literature by Veerendra *et al.,* [4] has a straightforward design and fewer components, but it has challenges in efficiently operating the drive motor. To get around these issues, a boost-type single-stage converter was suggested, which can produce three-phase voltage even from a DC input source having a low level. Single-stage charger for LEVs using a quadratic buck-boost AC-DC converter with a transformer less design has been designed but the absence of a Transformer limits the voltage gain for battery charging [5]. A two-stage 3.5kVA OBC for EVs with front-end and back-end converters has been introduced whose control strategy has 3 modes of charging but lacks the integration of bidirectional power flow capabilities for vehicle-to-grid applications [6]. Different topologies of converters have been proposed each being different from the other based on constraints like space of the supply device, efficiency of the converter, higher order harmonics, and PWM strategies for wide voltage range applications [7-9]. Additionally, numerous kinds of soft-switching approaches have been developed to reduce switching losses and increase converter efficiency [10-15].

To date, the proposed systems in the literature show complexity in operation and poor efficiency. For this reason, the primary focus of this paper was developing battery chargers for plug-in-charge electric vehicles. To sustain such EMS, a basic power electronic-based architecture is implemented. The charger's architecture is based on a bidirectional DC-DC converter, which increases system efficiency. Compared to the topologies found in the literature, the suggested DC-DC converter technique satisfies the required operation of the bi-directional charger in the energy management system. By regulating the voltage and current levels between the limits, the power electronic converters were made use to size the passive elements.

2. Proposed System

Figure 1 depicts the planned schematic of a fast EV charging station. Seamless system connectivity with renewable energy sources is made possible using a DC-DC converter and a DC bus. The DC bus voltage to EV battery voltage levels is maintained via an appropriate interleaved DC-DC converter. Several factors determine the total number of vehicles that can be charged, including the following: a) The parking space that is available for electric vehicles; b) The dire need for fast charging stations in a particular area. A comprehensive line diagram for the hybrid system which is proposed for usage used in EV charging applications is depicted in Figure 2.

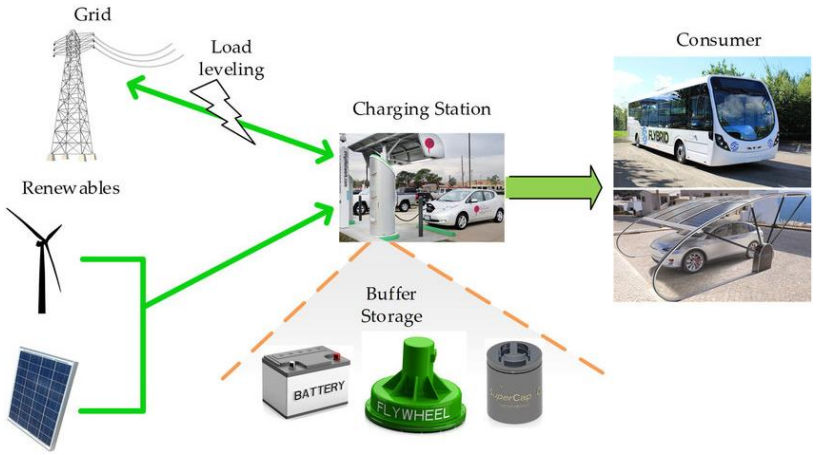

Fig. 1. Structure of Hybrid EV Charging Station

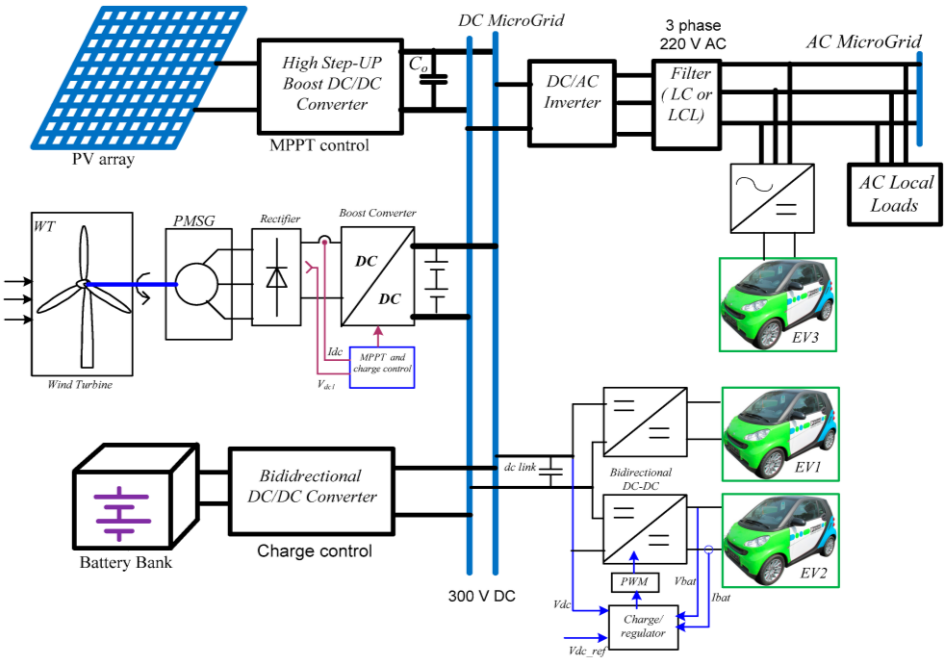

Fig. 2. Block diagram of proposed system

2.1 Electric Vehicle Structure

The use of electric vehicles is rising dramatically in the current situation. The overall structure of the electrical vehicle is depicted in the form of a block diagram in Figure 3. It's driven with electricity delivered to the motor. An electric vehicle is made up of several parts including power converters, electric motors, power converter control circuitry and batteries. Power converters aid in maintaining the correct amount of energy needed for motors and assist in controlling the battery's charging and discharging conditions.

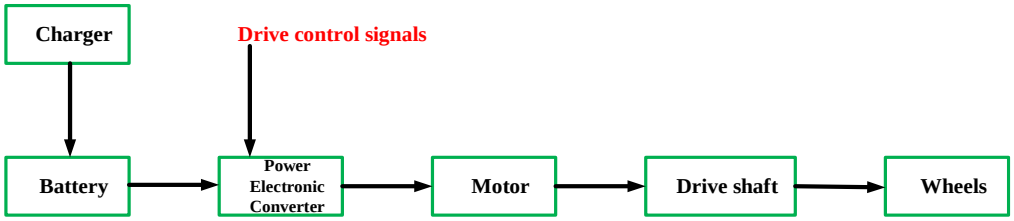

Fig. 3. Block diagram of EV

The motor drives the electric vehicle, as depicted in Figure 3. Additionally, it is made up of two converters: a PWM-based converter that aids in controlling the motor conditions, and a DC-DC bidirectional converter that controls the battery system's state of charge.

2.2 PV Solar System

Solar energy provides a renewable, environmentally friendly, and cost-effective source of electricity, promoting energy independence and reducing carbon emissions. Due to the photon effect, the solar panel converts sunlight into electrical energy. Solar cells first produce electric current, which is then converted into voltage through a similar electric circuit. The acquired DC voltage varies depending on the temperature of the sun and may harm electrical equipment. Figure 4 shows the circuit diagram for MPPT based PV system with a DC-DC converter. The main objective of MPPT is to ensure the solar panel's maximum output. To achieve the necessary voltage and current ratings, these cells were set up in series and parallel.

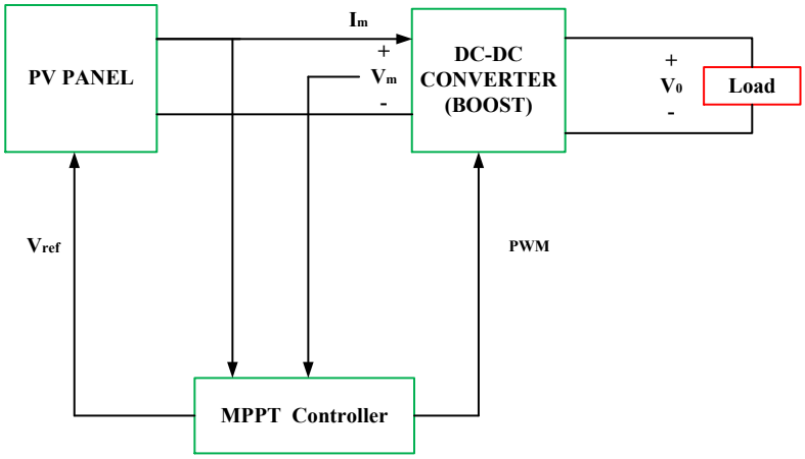

Fig. 4. PV system with power converter

2.3 Bio-Energy System

One of the many varied resources available to assist satisfy our energy needs is bioenergy. These systems are designed to convert biomass into usable energy forms, such as electricity, heat, or biofuels, through various methods like combustion, fermentation, or anaerobic digestion, as shown in Figure 5. Bioenergy systems offer several advantages for a country, contributing to energy sustainability, economic growth, and environmental stewardship. Some of the key benefits are reduction in carbon emissions, energy security, economic growth, rural development by job creation, waste reduction and resource recovery and many more.

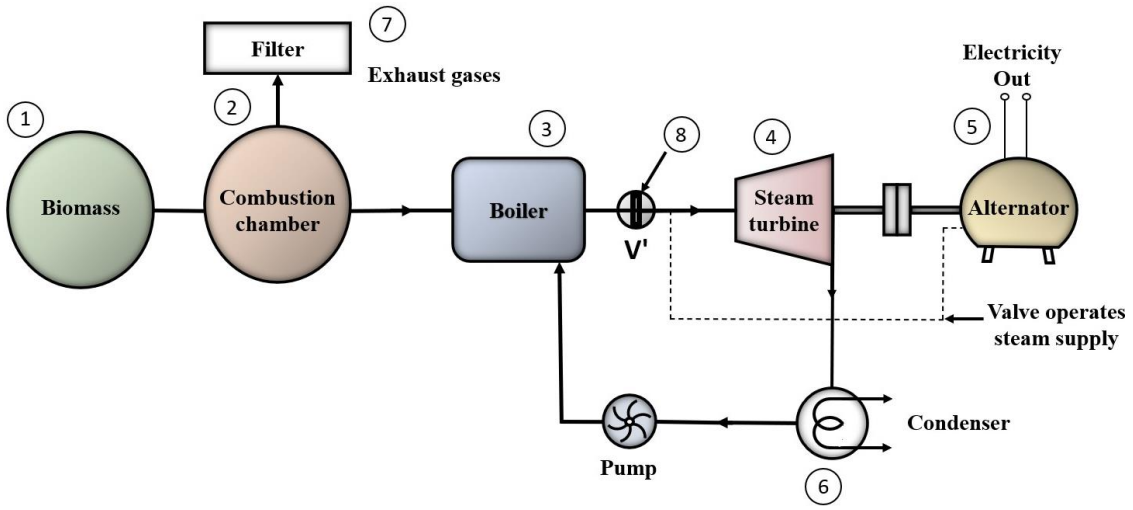

Fig. 5. Diagram of bioenergy system

2.4 Perturb and Observe MPPT Algorithm

Optimisation problems are a common occurrence in many different research and technological domains. Sometimes these challenges might be extremely complex because of the real and practical nature of objective function or the model limits. In a typical optimization issue, an objective function that is subjected to strong equality and/or equality limitations and complex, nonlinear properties is minimised or maximised.

When using the P&O approach, the system first tracks variations in the voltage of the PV array to ascertain the way the output power is altered. Figure 6 displays a P&O MPPT algorithm. The flowchart depicts the calculation of the PV power once the voltage and current of the PV panel have been determined.

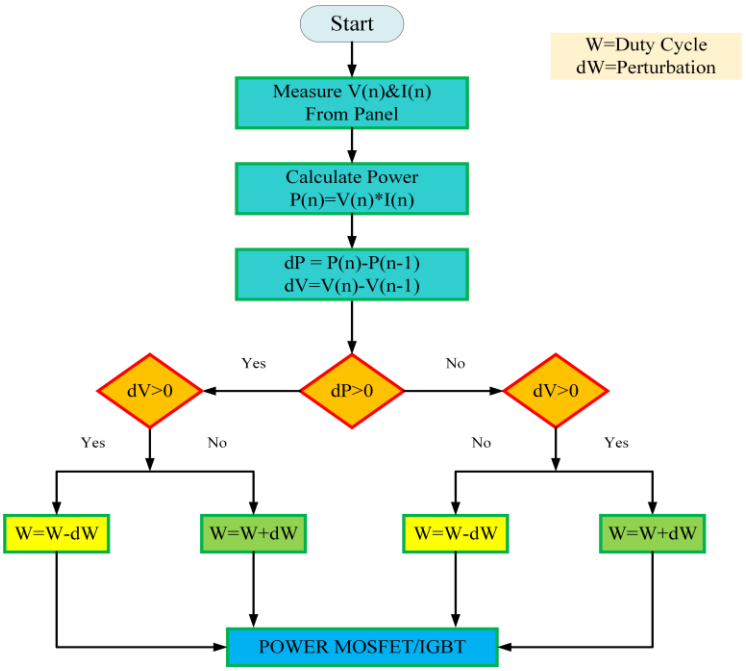

Fig. 6. Flowchart representation of P&O technique

2.5 DC-DC Converter

A minimum of one DC/DC converter is needed to interface super capacitor, fuel cell, or a battery with a common DC link, depending on the various EV topologies. The DC/DC converter can function as a step-up converter, raising, or as a step-down converter, lowering the low-level input voltage. In electric vehicles, to run low-level voltage components like dashboards, air conditioners, radios etc, step-down converters are needed. To run motors effectively, step-up converters are employed to raise the voltage levels to the needed.

A DC-DC bi-directional converter is shown in Figure 7, It is helpful for regenerative breaking and has bidirectional control of power. The duty cycle of a converter determines how much power is being controlled, and this is typically done to control the output current or the input and output voltages.

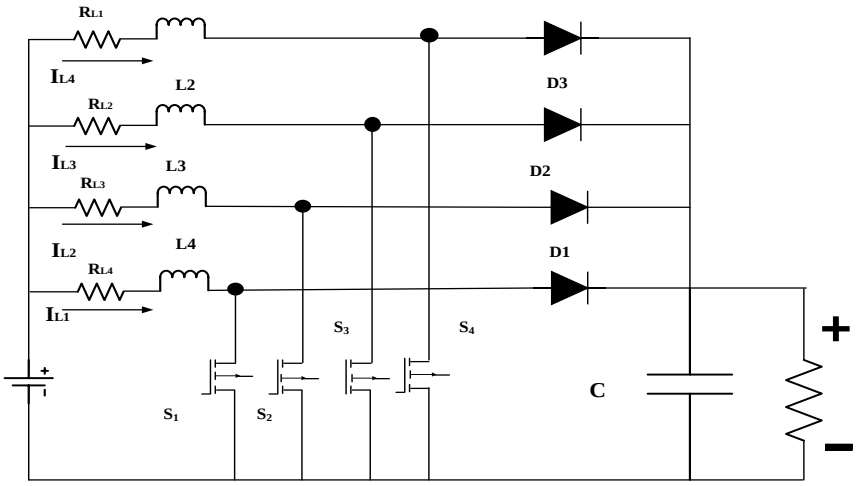

Fig. 7. FP-IBC

The four-phase interleaved boost converter as shown in Figure 8, consists of two diodes, four switches with series-connected inductors and two output filter capacitors. Four-phase interleaving is used in the topology. Each 104-phase circuit has a phase difference of 90 electrical degrees, increasing the output current frequency by 105 times and lowering the ripple after superposition. Additionally, the converter has a relatively high boost that satisfies the fundamental criteria for a conventional DC-DC converter.

Case 1: S_1 is ON (M1000) and other switches are OFF.

Here S1 closed and other switches open, as shown in Figure 8.

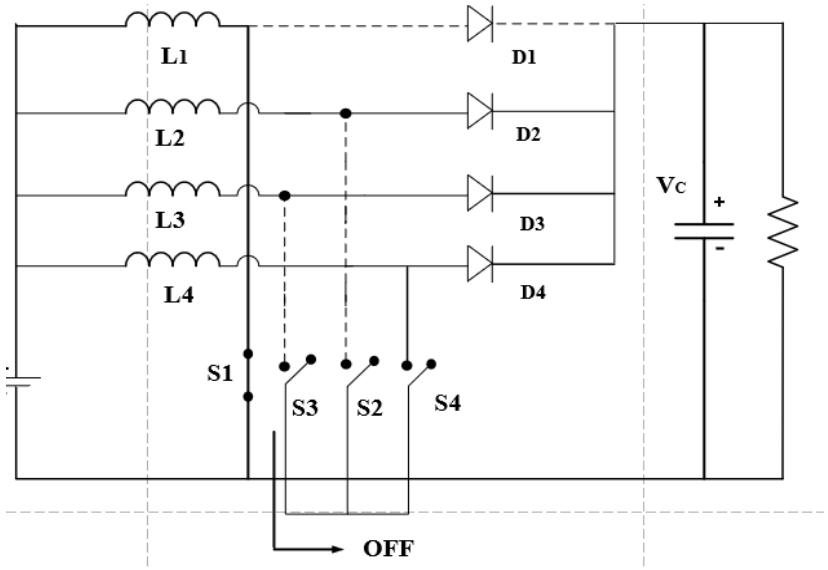

Fig. 8. Mode-1 Operational Diagram for Interleaved DC-DC Converter

A charging loop is created by the power source, the switch tube Q1, the inductor L1, and the power source. With the power supply and the two capacitors C1 and C2, along with the three diodes D2, D3, and D4 of the branch, the remaining three inductors, L2, L3, and L4, create three loops. The power supply, the load, the capacitors C1 and C2, and the final loop are R. Energy is provided to the load by capacitors C1 and C2 under the relationship depicted in Eq. (2).

$$\begin{aligned} L11\frac{di_{L11}(t)}{dt} &= +V_{in1}(t) \\ L_{2a(3,4)}\frac{di_{L2a(3,4)}(t)}{dt} &= -V_{outa}(t)+V_{ina}(t) \\ C\frac{dv_{outa}(t)}{dt} &= \sum_{i=2}^{4} i_{L1a}(t)-\frac{v_{outa}(t)}{R} \end{aligned} \tag{2}$$

The duty cycle, di(t) (i=1 to 4), can be used to calculate the opening time of each switch, di(t)Ts. The four-phase IBC operates under the premise that there should be a Ts/4 shift angle between every pair of adjacent phases, and that each phase's duty cycle should remain constant. Only eight work states can exist in a period when the sixteen possible work states are added together, and it is shown in Table 1 respectively as follows.

Table 1
Four-phase IBC Switching Conditions

Case	Condition	Working States
1	$0<dc_{1x}(t)+dc_{2x}(t)+dc_{3x}(t)+dc_{4x}(t)\leq 1$	dM1000→dM000→dM0100→dM0000→dM0010→dM0000→dM0001→dM0000
2	$1<dc_{1x}(t)+dc_{2x}(t)+dc_{3x}(t)+dc_{4x}(t)\leq 2$	dM1000→dM1100→dM0100→dM0110→dM0010→dM0011→dM0001→dM1001

3	$2<dc_{1x}(t)+dc_{2x}(t)+dc_{3x}(t)+dc_{4x}(t)\leq 3$	dM1011→dM1001→dM1101→dM1100→dM1110→dM0110→dM0111→dM0011
4	$3<dc_{1x}(t)+dc_{2x}(t)+dc_{3x}(t)+dc_{4x}(t)\leq 4$	dM0111→dM1111→dM1011→dM1111→dM1101→dM1111→dM1110→dM1111

By comparing the triangle waveforms Vtri i(i=1 to 4) and duty cycle Vcon i(i=1 to 4), one can obtain the driving waveforms Gi. Two neighbouring drive waveforms in case 4, as shown in Figure 9, have an interval time of TS/4, meaning that t1a+t2a=t3a+t4a=t5a+t6a=Ts/4. In example 4, at least three switches are closed simultaneously in a single period because of the high-duty cycle of each switch.

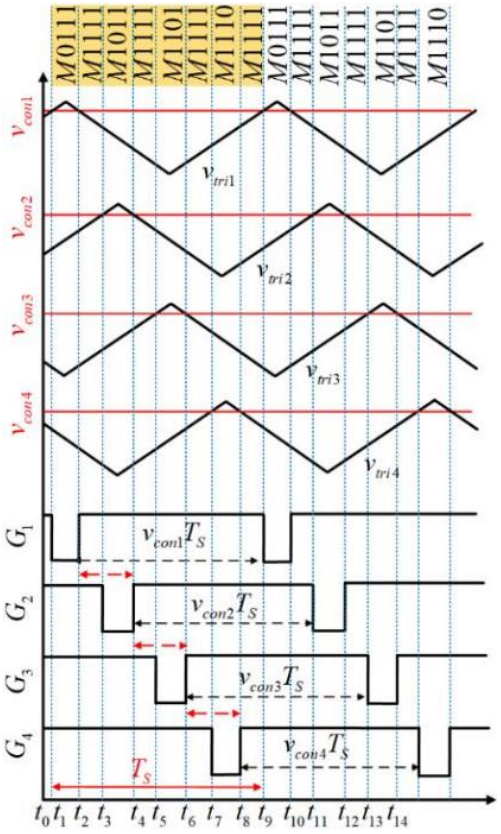

Fig. 9. Illustrated waveforms

2.6 Control Strategy For FP-IBC

The four-phase interleaved bidirectional controller's control scheme employs a traditional pulse width modulated approach. This PWM approach uses the signals from the output parameter and the input DC voltage/current to obtain the reference signal. Below is a time-lapse of the FP-IBC converter's fundamental switching pattern. In Figure 10, Four switches have a switching time of Ts. The general phase shift of any phase can be determined via the expression below:

The phase shift = Ts/ (number of parallel phases*number of switches in phase)

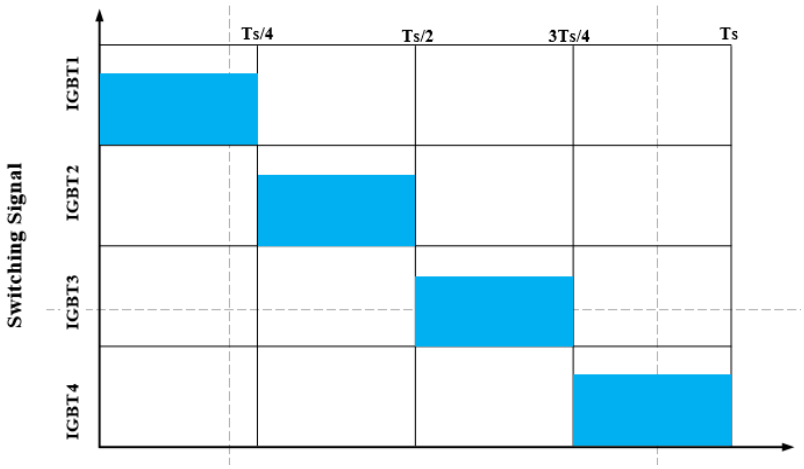

Fig. 10. Switching sequence

For example, in FP-IBC, a higher number of parallel branches will raise the power rating and reliability of the converter, as shown in Figure 11. As power is observed at the output and the frequency is four times the standard switching frequency, it leads to distribution losses and semiconductor device sizing. In contrast to traditional DC/DC converters like MDBC and BC, FP-IBC offers the following benefits for EVs.

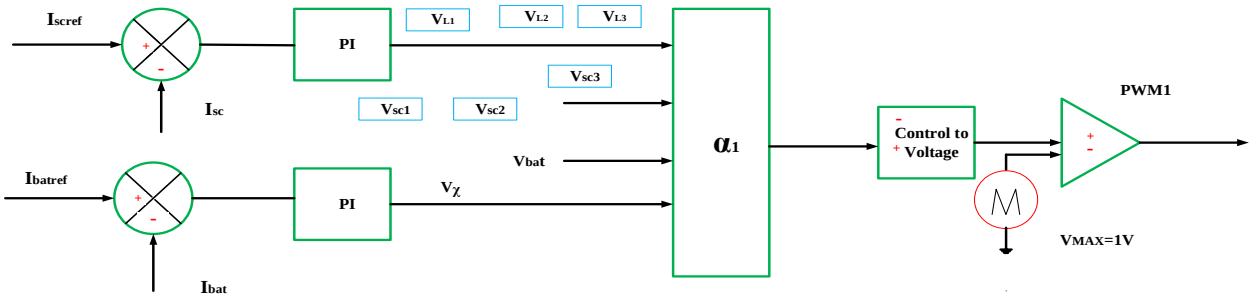

Fig. 11. Control diagram for DC-DC FP-IBC converter

The expression for the calculation of the effective duty cycle is shown below.

$$D_{eff} = 1-(V_{in}/V_o)^{1/2} \tag{3}$$

$$I_o = (1-D_{eff})^2.I_{L1} \tag{4}$$

The required minimum delay time for proper ZVT operation is.

$$t_d \geq \frac{i_{L2}.L_r}{V_o} + \frac{\Pi}{2}\sqrt{L_r.C_s} \tag{5}$$

The expression for input and output power of dc-dc converter is shown as

$$P_{IN} = P_{SWITCH} + P_{DIODE} + P_{INDUCTOR} + P_{OUT} \tag{6}$$

$P_{out} = V_o * I_o$

3. Simulation Analysis

MATLAB/Simulink is used to analyse the performance of a four-phase interleaved boost converter with an inductor that is powered by a grid-connected PV-Bio hybrid system. The results are illustrated. Table 2, Table 3, and Table 4 depict the specifications required for PV, FP-IBC, and bioenergy systems respectively.

Table 2
PV system specifications

Parameters	Ratings
Power	1500W
Panel max Voltage	220V
Panel max Current	6.818A
Voc	232.32V
Isc	5.65A
No. of panels	10
No. of strings	1

Table 3
FP-IB converter specifications

Parameters	Ratings
Input voltage (V)	100
Inductor(μH)	578.2
Capacitor(μF)	100
Switching Frequency (kHz)	25

Table 4
Bio-plant system specifications

Parameters	Ratings
Maximum Power (W)	5000
Peak power (W)	6800
Rated Voltage	415
Rated Rotor Speed (RPM)	250
Generator Type	SCIG

Case 1: Analysis of PV-Bio Hybrid System for Load Sharing

According to the modelling expressions shown in the preceding parts, the solar and bio systems in this are designed. The bio energy system is intended to produce 5kw, and the solar plant is intended to produce 15kw. The power management approach for various load conditions is displayed.

Figure 12 displays the simulation output for the proposed system in addition to the power management strategies used along with P&O based MPPT controller. Here, the PV, battery, and grid systems are chosen for load sharing based on their respective generations.

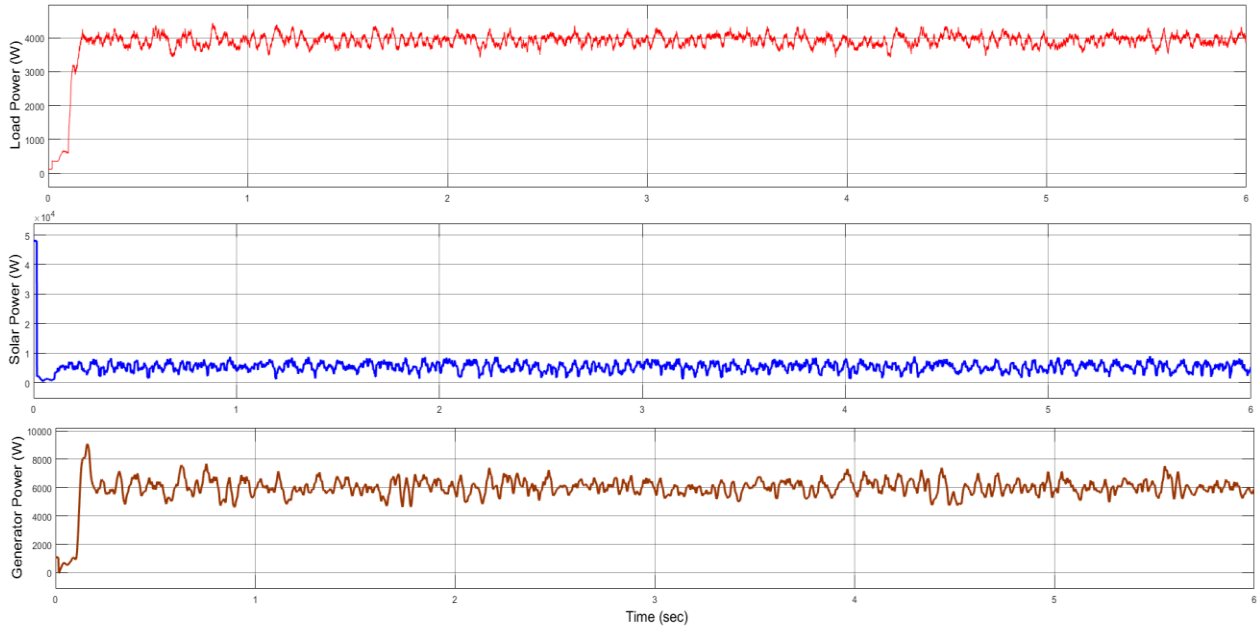

Fig. 12. Output of (a) Load Power, (b) Solar Power, (c) Bio Power using P&O MPPT

Figure 13 shows the simulation results which shows the grid voltage and current.

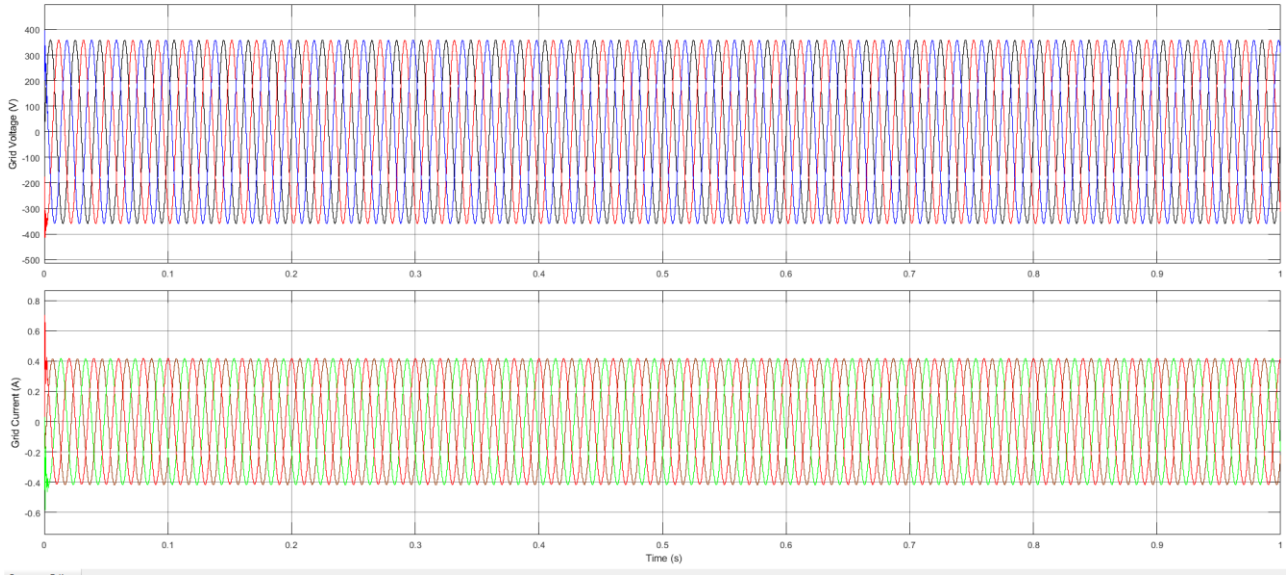

Fig. 13. Simulation result for Grid Voltage and Current

Figure 14 displays the results of the simulation, indicating the PV voltage and current needed to match the load requirement. In this instance, power management circumstances are noted while the electric vehicle is operating.

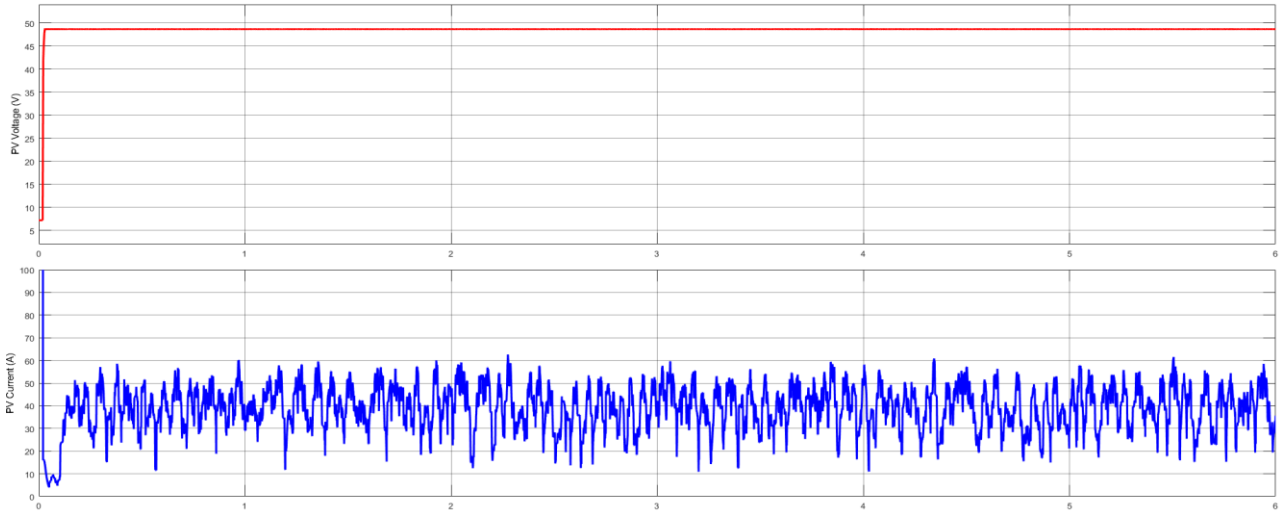

Fig. 14. Simulation result for PV voltage and current

In this case, as illustrated in Figure 15, the simulation results indicate that the DC voltage and current through biowaste satisfy the load demand. During this case, the total harmonic distortions for load voltage and current is shown below.

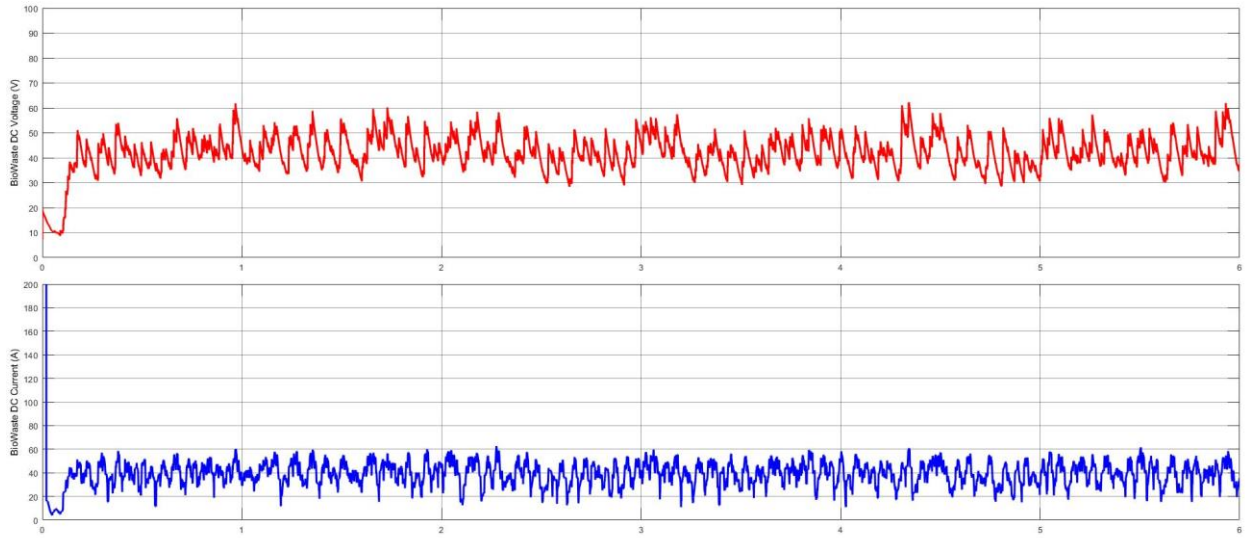

Fig. 15. Simulation result for bio waste DC voltage and current

Figure 16 and Figure 17 show total harmonic distortions for load voltage and load current under operating different load conditions.

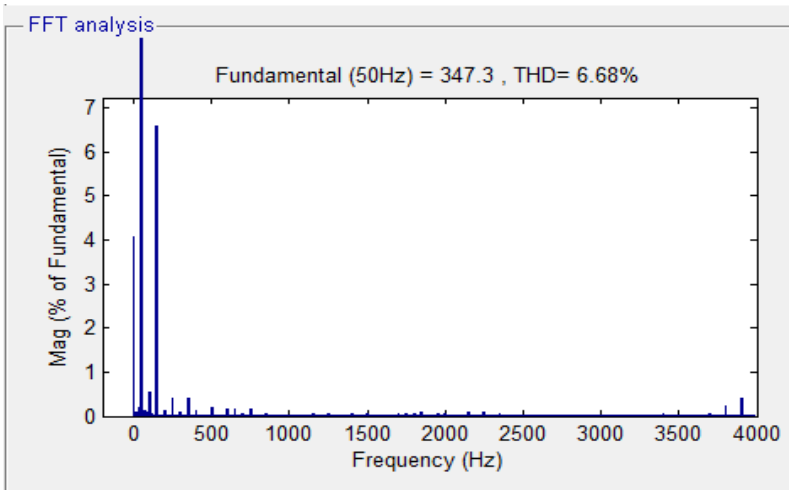

Fig. 16. Harmonic Analysis for Load current

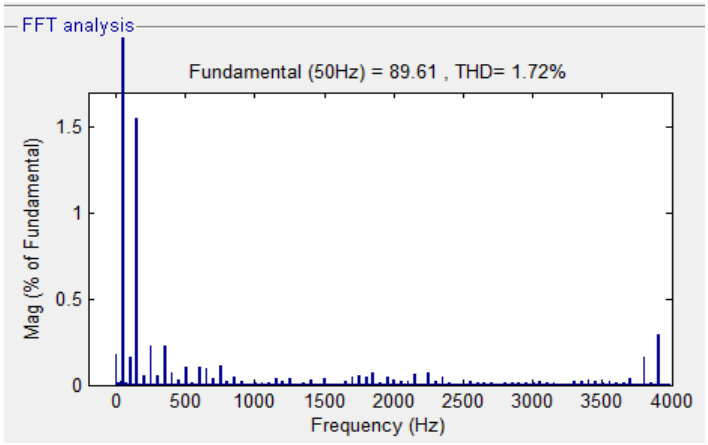

Fig. 17. Harmonic Analysis for Load Voltage

Case 2: Analysis of proposed hybrid system for EV charging Conditions

In this case, a grid-connected hybrid PV and bioenergy system is used to build a charging station. MATLAB simulates the modelling of the EV charging system. The primary objective of the simulation is to evaluate how well the conventional algorithm performs under various operating conditions to provide a continuous charging procedure at a fixed or reduced price. These tests are typically carried out for continuous charging at a fixed charging rate.

The simulated waveforms of system powers, when an electric vehicle with a 5kW load capacity is connected to a charging station, have been shown in Figure 18. The PV-Bio hybrid system provides the energy needed to charge the electric car, with the remaining energy being stored in the batteries. The graphics below display the voltage and current waveforms for DC-DC interleaved converters.

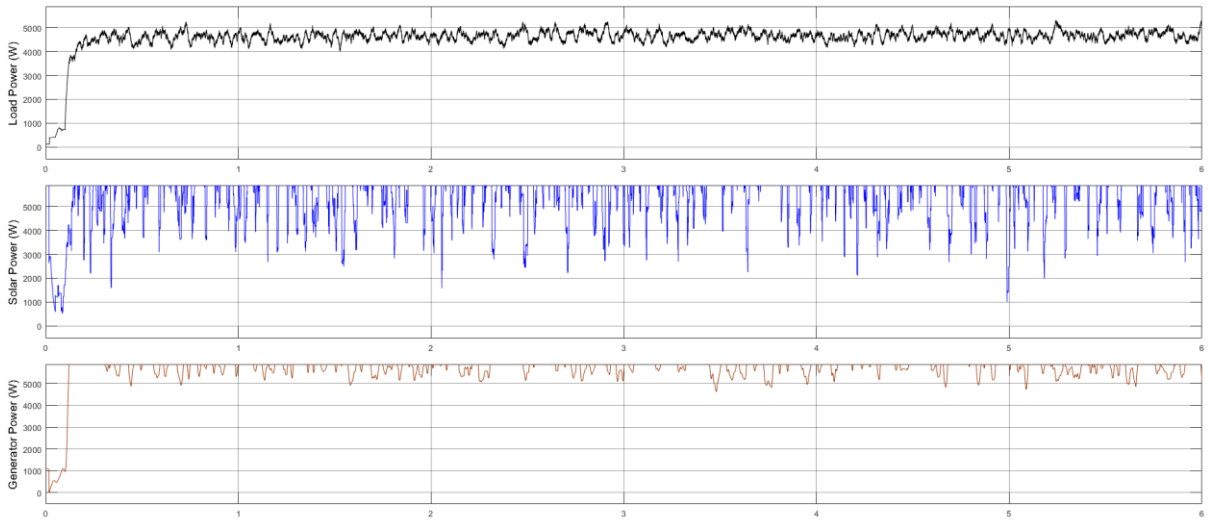

Fig. 18. Simulation waveform for system powers

The voltage and current waveform of an interleaved DC-DC converter are shown in Figure 19. Here, the converter's goal is to preserve EVs' ability to charge quickly. It can do this by continuing to produce large output currents—nearly 400 amps—from the converter. To attain a high current from the converter, appropriate parameters for the inductors are examined. Additionally, the suggested modulation approaches aid in preserving the correct order of the switches in an interleaved DC-DC converter. The 3kW battery-based electric vehicle requires over 3 hours and 25 minutes to get a full charge at our current rate. Figure 20 displays the battery state of charge conditions for electric vehicles. This EV battery takes 55 minutes to charge to 25% capacity. It takes an additional 50 minutes to reach 25–80% charge, and it takes an additional 40 minutes to finish charging.

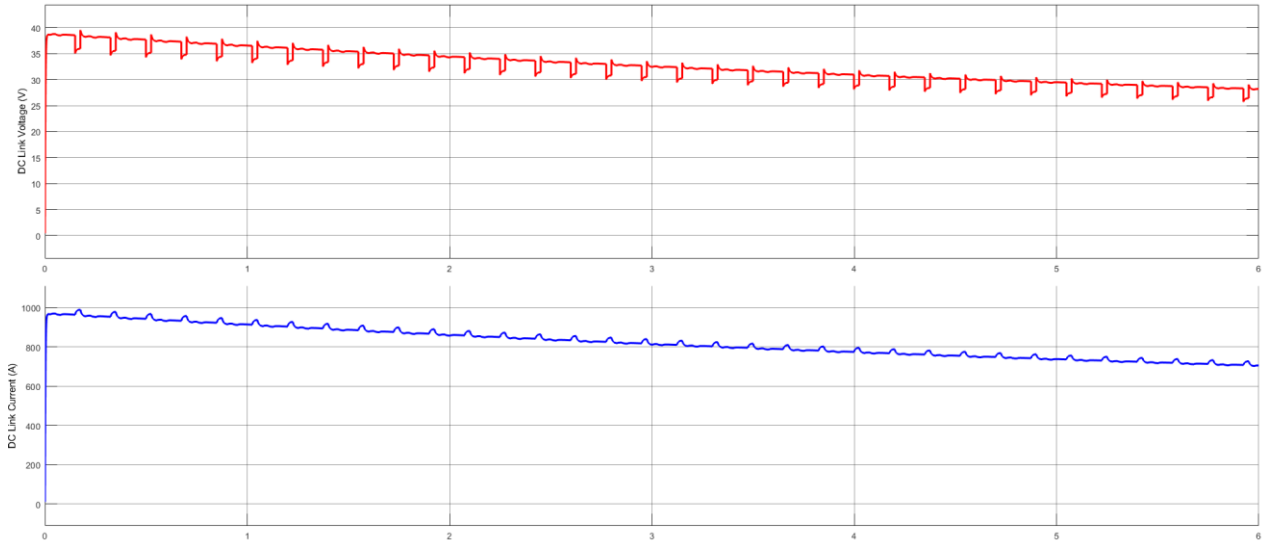

Fig. 19. Simulation output of Voltage and current of DC-DC converter

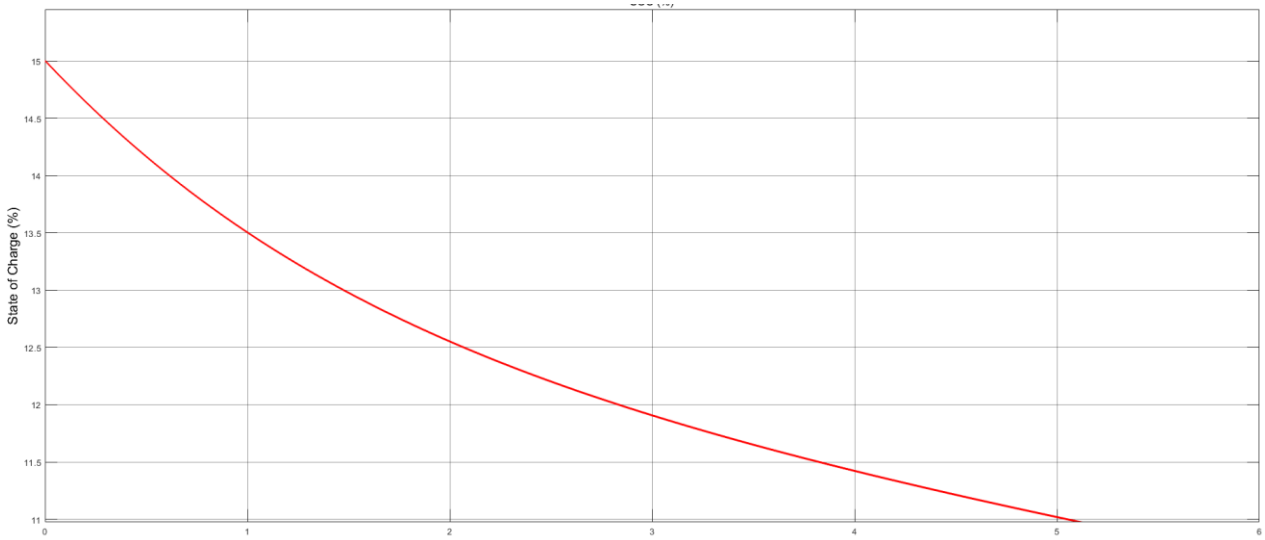

Fig. 20. EV Battery Charging Conditions

4. Conclusions

This paper proposes an effective control scheme for an interleaved DC-DC converter, which lowers voltage ripples that increase the EV charging station's efficiency. Two requirements have been verified for the proposed control: first, a reduction in voltage ripples. Simulation findings show that the proposed interleaved converter produces voltage ripples of 3.84% compared to 5.12% for the standard boost converter. Additionally, this research suggested an interleaved boost converter for EVs that require quick charging. According to the battery's SOC level, the converter's phases are controlled to maintain a nearly 98% efficiency in the fast-charging region. The three charging speeds are slow (0–20% SOC level), quick (15-20% SOC level), and medium (80–100% SOC level). The battery life is extended by using these modes. The paper includes the analysis and simulation findings. To fully charge the car, 145 minutes are needed. Additionally, the converter runs in constant voltage mode for quick charging. In order to charge the EV as efficiently as possible, this article optimises the usage of the phases of the proposed interleaved converter. As a result, this will be a practical and economical rapid charging station option.

Acknowledgement
No funding was received for conducting this study.

References

[1] Veerendra, Arigela Satya, Mohd Rusllim Bin Mohamed, and Fausto Pedro García Márquez. "Energy management control strategies for energy storage systems of hybrid electric vehicle: A review." *Energy Storage* 6, no. 1 (2024): e573. https://doi.org/10.1002/est2.573

[2] Inampudi, Prasanna Kumar, Chandrasekar Perumal, Venkata Ramana Guntreddi, and Tadanki Vijay Muni. "A Novel DC-DC Boost Converter with Coupled Inductors for High Gain and Smooth Switching." *Journal of Advanced Research in Applied Sciences and Engineering Technology* 48, no. 2 (2024): 92-104. https://doi.org/10.37934/araset.48.2.92104

[3] Ahmad, Fareed, and Mohd Bilal. "A Comprehensive Analysis of Electric Vehicle Charging Infrastructure, Standards, Policies, Aggregators and Challenges for the Indian Market." *Energy Sources, Part A: Recovery, Utilization, and Environmental Effects* 45, no. 3 (2023): 8601-8622. https://doi.org/10.1080/15567036.2023.2228734

[4] Veerendra, Arigela Satya, Mohd Rusllim Mohamed, and Chavali Punya Sekhar. "Modelling and analysis of voltage balancing topology for series-connected supercapacitor energy storage system." *International Journal of Modelling and Simulation* 44, no. 5 (2024): 329-342. https://doi.org/10.1080/02286203.2023.2183464

[5] Abd Aziz, Mohd Azri, Mohd Saifizi Saidon, Muhammad Izuan Fahmi Romli, Siti Marhainis Othman, Wan Azani Mustafa, Mohd Rizal Manan, and Muhammad Zaid Aihsan. "A review on BLDC motor application in electric vehicle (EV) using battery, supercapacitor and hybrid energy storage system: efficiency and future prospects." *Journal of Advanced Research in Applied Sciences and Engineering Technology* 30, no. 2 (2023): 41-59. https://doi.org/10.37934/araset.30.2.4159

[6] Abdelmomen, Mahmoud Sameh, Ibrahim Abdelsalam, and Mostafa S. Hamad. "Two-Stage Single-Phase EV On-Board Charger Based on Interleaved Bridgeless AC-DC Converter." In *2023 5th International Youth Conference on Radio Electronics, Electrical and Power Engineering (REEPE)*, vol. 5, pp. 1-6. IEEE, 2023.

[7] Naaz, Maliha, Kaleem Fatima, B. Rajendra Naik, Mohammad Ibrahim, Asfiya Jabeen, and Syed Junaid Hussain. "A DC-DC Boost Converter using PWM with 65% efficiency." In *2023 IEEE Devices for Integrated Circuit (DevIC)*, pp. 377-382. IEEE, 2023. https://doi.org/10.1109/DevIC57758.2023.10134808

[8] Hu, Song, Xiaodong Li, and Qing-Fei Zheng. "A dual-bridge DC-DC resonant converter using extended PWM and phase-shift control." *IEEE Transactions on Industry Applications* 57, no. 4 (2021): 4009-4020. https://doi.org/10.1109/TIA.2021.3072018

[9] Wang, Jiangfeng, Hongfei Wu, Tianyu Yang, Li Zhang, and Yan Xing. "Bidirectional three-phase DC-AC converter with embedded DC-DC converter and carrier-based PWM strategy for wide voltage range applications." *IEEE Transactions on Industrial Electronics* 66, no. 6 (2018): 4144-4155. https://doi.org/10.1109/TIE.2018.2866080

[10] Hasanpour, Sara, Yam P. Siwakoti, and Frede Blaabjerg. "A new soft-switched high step-up trans-inverse DC/DC converter based on built-in transformer." *IEEE Open Journal of Power Electronics* 4 (2023): 381-394. https://doi.org/10.1109/OJPEL.2023.3275651

[11] Kalahasthi, Rajesh Babu, Manojkumar R. Ramteke, Hiralal Murlidhar Suryawanshi, and Koteswara Rao Kothapalli. "A high gain soft switched DC-DC converter for renewable applications." *International Journal of Electronics* 110, no. 8 (2023): 1447-1467. https://doi.org/10.1080/00207217.2022.2117423

[12] Madiseh, Nasrin Asadi, Ehsan Adib, and Mohammad Reza Amini. "A Novel Soft Switching Non-Isolated Bidirectional dc-dc Converter Without Any Extra Auxiliary Switch." *IEEE Journal of Emerging and Selected Topics in Power Electronics* 12, no. 2 (2023): 1875-1882. https://doi.org/10.1109/JESTPE.2023.3250435

[13] Rao, Podila Purna Chandra, Radhakrishnan Anandhakumar, and L. Shanmukha Rao. "Analysis of a novel soft switching bidirectional DC-DC converter for electric vehicle." *Bulletin of Electrical Engineering and Informatics* 12, no. 5 (2023): 2665-2672. https://doi.org/10.11591/eei.v12i5.4505

[14] Swain, Sarthaak Rohan, Shiva Kumar Sarode, and Ayyagari Sai Lalitha. "Soft Switching Dual Active Bridge Converter for Electric Vehicle Charging Infrastructure on Dual Load Application." In *2024 Third International Conference on Power, Control and Computing Technologies (ICPC2T)*, pp. 168-172. IEEE, 2024. https://doi.org/10.1109/ICPC2T60072.2024.10474804

[15] Rao, J. V. G. Rama, and S. Venkateshwarlu. "Soft-switching dual active bridge converter-based bidirectional on-board charger for electric vehicles under vehicle-to-grid and grid-to-vehicle control optimization." *Journal of Engineering and Applied Science* 71, no. 1 (2024): 49. https://doi.org/10.1186/s44147-024-00384-z